Attaining neoclassical transport in ignited tokamaks

M. Kotschenreuther[†], W. Dorland[1], Q. P. Liu[†], M. Zarnstorff[2], R. L. Miller[3], Y. R. Lin-Liu[3]

[†]Institute for Fusion Studies, The University of Texas, Austin, TX, 78712

[1]Institute for Plasma Physics, University of Maryland, College Park, MD, 20742

[2]Princeton Plasma Physics Laboratory, P. O. Box 451, Princeton, NJ, 08543

[3]General Atomics, P. O. Box 85608, San Diego, CA, 92138-5608

Abstract

The requirements to stabilize microinstabilities with velocity shear in tokamaks are examined for both aspect ratio $A = 3$ and $A = 1.4$. A comprehensive linear gyrokinetic code is used to compute growth rates in realistic numerical equilibria. Growth rates for $A = 3$ and $A = 1.4$ are generally similar for electron drift modes and ion temperature gradient (ITG) modes. Velocity shear is stronger at low aspect ratio; however, low A profiles have a stronger microtearing mode which is more difficult to shear stabilize. Nonetheless, low aspect ratio devices are predicted to have good confinement and may ignite at very small size. Profiles are presented which may allow high β, MHD-stable operation at $A = 1.4$ with high confinement. The possibility of using a controlled application of non-turbulent loss processes to control profiles to prevent turbulent transport and to maximize β is suggested.

I. INTRODUCTION

Recent experimental results [1] indicate that it is possible to reduce turbulence levels and transport to neoclassical levels over some region of the plasma, termed a transport barrier. Such improvements in confinement are very important, because they could allow ignition devices which are much smaller and less expensive than would be necessary in a fully turbulent plasma without any transport barriers (i.e. an L-mode). Theoretical and experimental evidence indicates that turbulence suppression is due to velocity shear [2] as well as magnetic geometry [3,4], though important aspects of this process are not well understood. In the present work we use current theoretical understanding of turbulence suppression to predict the optimum conditions for confinement in tokamaks. These conditions could be the basis of small ignited tokamak plasmas. A feature of the present work is an exploration of the effects of magnetic geometry on instabilities and the velocity shearing rate, using a comprehensive calculation of the short wavelength gyrokinetic instabilities. Particular emphasis will be placed on comparisons of standard aspect ratio ($A = 3$) and low aspect ratio ($A = 1.4$) tokamaks.

II. METHODS

We make use of the paradigm developed by many authors [1,3,5], which indicates that turbulence is strongly suppressed when the $\boldsymbol{E} \times \boldsymbol{B}$ shearing rate exceeds the growth rate for toroidal ITG and drift modes. To obtain the growth rate to apply this criterion, a comprehensive, linear, initial-value, electromagnetic, gyrokinetic code is used. The code generalizes previous electromagnetic algorithms [6] to include all the electromagnetic fields in a gyrokinetic instability: the electrostatic potential ϕ, the parallel vector potential $A_\parallel$ and the magnetic field compression $\delta B_\parallel$. The gyrokinetic equation is solved in the eikonal (ballooning) limit [7] with all kinetic effects. The code describes ion temperature gradient driven (ITG) modes, electron drift modes, ideal and linear kinetic ballooning modes, micro-

tearing modes, and any other linear instability of the gyrokinetic equations. The initial value code automatically finds the most unstable mode by running long enough in time. It has been benchmarked against two other gyrokinetic eigenvalue codes [6], in one case with full geometry and electromagnetic effects. The magnetic geometry is found from a numerical solution of the Grad-Shafranov equation using the program TOQ [8,9].

III. RESULTS

Practical fusion applications require as high a β as possible. Therefore, in the comparisons which follow we use pressure profiles which are close to the ideal ballooning limit. To determine this, the pressure profile is specified as a function of the normalized poloidal flux $\overline{\psi}$ times an arbitrary constant. The constant is varied to be slightly less ($\sim 5-20\%$) than the value at which an ideal ballooning mode first appears at one point in the minor radius in the numerical equilibria. Results from the profile as a whole are not sensitive to the exact margin below the ideal ballooning threshold.

The effect of collisions on the cases below is found to be slightly to modestly stabilizing (except very near the edge where collisionality is high). Collisional effects also do not change the trends below. For space we only present only *collisionless* cases here; then the normalized growth rates are the same whether A was changed by varying minor radius or major radius, or whether β was changed by varying density or B field. The neglect of collisions is a pessimistic assumption, so if the shearing rate exceeds the growth rate presented here, it should exceed the growth rate including collisions. For simplicity we take $\eta = d\ln T/d\ln n = 1$, and $T_i/T_e = 1$. Larger η increases the growth rates by up to a factor of roughly η, but does not change the qualitative trends. Cases with large density gradients such as these probably correspond to experiments with core fueling, as by pellet injection.

The diamagnetic shearing rate is computed using the Hahm-Burrell formula [2] evaluated at the outer midplane, assuming enE_r exactly balances the ion pressure gradient, as would be roughly true in an ignited plasma without external momentum inputs. This balance is

only an approximate estimate to the neoclassical results. Recent measurements [10] have shown some discrepancies between measured flow velocities and neoclassical predictions, so we choose the estimate based on simple physical reasoning and note there is uncertainty on this issue. In neoclassical theory, the density gradient and temperature gradient parts of the pressure gradient contribute differently to E_r. The density gradient contribution is as described here; however, temperature gradients contribute less to E_r. For $A = 3$, the temperature gradient contribution is roughly half what is described here, so the total E_r (from both density and temperature gradients) would be reduced by roughly a quarter. For $A = 1.4$, however, temperature gradients contribute nearly equally with density gradients to E_r except near the axis, so the discrepancy is small. (This occurs because the ratio of the trapped particle fraction to the passing particle fraction is quite large in these equilibria, $\sim 5 - 10$ in the outer half, so the results of Ref. [11] imply that the poloidal flow is small in the banana regime.)

In Fig. 1, we compare cases with $A = 1.4$ and $A = 3$ which are otherwise nearly identical, and which have simple current and pressure profiles. Both have elongation $\kappa = 2.5$, triangularity $\delta = 0.5$, and the same functional forms for current J and pressure p: $J = J_0(1 - \psi)$ and $p = p_0(1 - \psi^2)$. The constant J_0 is adjusted so both have $q_{95} = 4.55$. Both are close to their respective beta limits, with $\langle\beta\rangle = 4.5\%$ for $A = 3$ and $\langle\beta\rangle = 27\%$ for $A = 1.4$. Scaling properties of the gyrokinetic equation show that v_{th}/L (where L is the pressure scale length and v_{th} is the local ion thermal speed) is an appropriate normalization for the growth rate γ, and $\rho_i^2 v_{th}/L$ is an appropriate normalization for the diffusivity χ and D_m, a linear approximation [12] to χ.

There is no substantial difference in the magnitude of the maximum growth rates and the D_m between $A = 3$ and $A = 1.4$ for modes with $k_\theta \rho_i < 1$, or in the extent of the minor radius over which the instability is present. We find that this result is typical when one compares cases which are at a comparable and large fraction of the ideal MHD β limit. Previous comparisons of kinetic drift instabilities [13] at different aspect ratios have not related β in this way.

We find that the current profile is a much stronger factor than aspect ratio in determining $\gamma/(v_{th}/L)$. Figures 2–3 show current profile scans (at constant total current) for both $A = 3$ and $A = 1.4$. The current and pressure profiles for both $A = 3$ and $A = 1.4$ use $J = J_0\,(1 - \psi^2 + J_2(\psi^2 - \psi^3))$, where increasing J_2 makes the current more hollow, and J_0 is adjusted to keep I/aB a constant equal to 1.4 and 5.6 for $A = 3$ and $A = 1.4$, respectively. The functional form of the pressure profile is also kept fixed ($dp/d\psi = .025 + .975\psi - \psi^2$), and the central beta is kept fixed at 10.5% and 60% for $A = 3$ and 1.4, respectively. For these runs $\kappa = 2$ for $A = 3$ and $A = 1.4$, $\delta = .5$ for $A = 1.4$, and $\delta = 0.8$ for $A = 3$ (which might be required for kink mode stability since $\beta_N = 4.7$ for the most hollow current profile).

Increasingly hollow current profiles reduce the growth rates of modes with $k_\theta \rho_i \leq 1$ by about an order of magnitude. Note that D_m decreases by a similar factor. Again, γ and the trends in γ are roughly comparable for $A = 3$ and $A = 1.4$, and the instabilities with the largest growth rate shift to larger $k_\theta \rho_i$.

The diamagnetic velocity shear (normalized to v_{th}/L) explicitly scales as ρ_*. For a central $\rho_* = .01$ (defined as the gyroradius evaluated with the central ion temperature and the vacuum toroidal field, divided by the horizontal minor radius) the shearing rates of $A = 3$ and $A = 1.4$ are also comparable and strongly increase with hollowness of the current profile. This latter effect is due to increasing Shafranov shift [4]. Thus, hollow current profiles can cause the shearing rate to greatly exceed the growth rate.

Note that for the particular choice made here, where both the pressure gradient is split evenly between temperature and density, and where enE_r exactly balances the pressure gradient, the velocity shear goes to zero at the edge of the plasma. Removal of either of these assumptions results in finite velocity shear approaching the boundary.

The behavior of microinstabilities can be clarified varying the local equilibrium gradients and magnetic shear. However, it is necessary correct the MHD equilibrium consistently for this. A formalism for this was first developed by Greene and Chance [14] and is widely employed to examine second stability of MHD ballooning modes. We have used a functionally equivalent formulation [15] to examine similar behavior for microinstabilities.

A full presentation is found in [16]; space limits discussion to a single example: in Fig. 4 we obtain the growth rate as the equilibrium gradient scale length is varied (but keeping all other parameters fixed, such as β, magnetic shear, etc.) for the $A = 3$ hollow current profile cases in Fig. 2. It can be seen that as the gradient increases past a certain point the growth rate *decreases*, as does D_m. This is very similar to MHD second stability behavior, and seems more pronounced with hollow current profiles. The mode does not become stable; however, it becomes easier to stabilize with velocity shear. $A = 1.4$ cases are similar.

Such behavior for trapped electron modes in TFTR was found by Beer [4], using the analytic s-alpha model, and some numerical equilibria. However $\delta B_\parallel$ was not included, so stabilization may have been overestimated because of the increasing local magnetic well, as explained below. Using the methods outlined, we find similar behavior for ITG modes, including $\delta B_\parallel$.

It is found that the effect of magnetic shear on low $k_\theta \rho_i$ modes is weak for numerically generated equilibria. This is unlike the results of calculations used with the the s-alpha model. However, beta gradient effects such as the Shafranov [4] shift become stronger with more hollow current profile.

We point out that it is important to include electromagnetic effects, particularly the compressional effects. As pointed out by Berk and Dominguez [17,18], including $\delta B_\parallel$ cancels the stabilizing influence of the "self-dug" magnetic well for drift instabilities. Our numerical results corroborate their findings, and show that neglect of $\delta B_\parallel$ for $A = 3$ and $A = 1.4$ for these cases leads to an underestimate of the growth rate by factors of two to an order of magnitude or more. Analyses of advanced tokamak cases at both $A = 1.4$ and $A = 3$ have frequently neglected this effect [19], probably leading to a substantial underestimate of instability strength.

However, artificially eliminating $A_\parallel$ from the calculations in Fig. 2 results in little change in the growth rates for modes [other than the microtearing mode in Fig. 3]. The coupling to Alfvén waves and MHD ballooning modes occurs through $A_\parallel$, so we conclude that these modes are not kinetic MHD modes, but rather they are relatives of the usual low beta

electrostatic ITG/drift modes which require $\delta B_\parallel$ to eliminate self-dug well effects. The microtearing mode is found only in strongly hollow current profiles, (more frequently at $A = 1.4$ than $A = 3$). It is almost purely magnetic, since the frequency is nearly unchanged when ϕ and $\delta B_\parallel$ are artificially suppressed. It is driven only by electron temperature gradients and causes transport almost entirely in that channel.

The similarity of the size of the growth rates and the normalized D_m for $A = 1.4$ and $A = 3$ has substantial implications. The parameters of proposed volume neutron sources (with low to moderate energy multiplication Q) have $\rho_* \sim 1/50$, whereas proposed $A \sim 3$ devices with high energy gain have $\rho_* \sim 1/200 - 1/400$. (The high ρ_* of $A = 1.4$ cases derives from high beta values at low A, which implies low magnetic fields.) For levels of velocity shear which arise without external momentum sources, the velocity shear $\gamma_E \sim v_{th}\rho_i/L^2$, where L is the pressure gradient scale length. The ratio of growth rate to shearing rate therefore scales as ρ_*, so that low aspect ratio devices have significantly greater potential for velocity shear stabilization.

Without velocity shear stabilization, the $A = 1.4$ case is at a substantial disadvantage. A rough estimate of the global confinement time is $\tau \sim a^2/\chi$. Assuming $\chi \sim C\rho_i^2 v_{th}/L$, one finds $\tau \sim (a/v_{th})(L/a)\rho_*^{-2}$. Presuming both $A = 1.4$ and $A = 3$ devices operate at roughly the same temperature (*i.e.*, $15 - 25$KeV) and have roughly the same profile effects (*i.e.*, a/L is comparable), then the strong ρ_* dependence puts the $A = 1.4$ device at a one to two order of magnitude disadvantage. (Note that the density of both proposed volume neutron sources and $A = 3$ burning plasma devices are typically also similar to within a factor of two.) The results here indicate that there is no strong aspect ratio dependence to the coefficient C to overcome this, if velocity shear is neglected. Therefore, the relative attractiveness of low A devices to obtain high confinement is strongly linked to their potential for velocity shear stabilization.

Attractive tokamak reactor operating modes have a very high fraction of bootstrap current and thus hollow current profiles. We have therefore examined equilibria with very high bootstrap fractions ($> 90\%$) at $A = 3$ and $A = 1.4$. In each case we used a functional form for

p which had previously been found to give high β with MHD stability [20] to both kink modes (with a conducting shell at $b/a = 1.3$) and ballooning modes: $dp/d\psi = .025 + .975\psi^3 - \psi^4$. Results are shown in Fig. 5, for values of ρ_* typical of proposed burning plasma devices.

Both cases satisfy the velocity shear stabilization criterion to drift/ITG modes with $k_\theta \rho_i < 1$ at all minor radii, and both cases fail to satisfy that criterion in the center for the high k modes (microtearing modes). Note that for $A = 1.4$ the shearing rate exceeds the growth rate by a very large margin towards the edge. This margin exceeds the uncertainties in the calculation of E_r noted previously.

We believe the main uncertainty in these results lies in the possibility of nonlinear instabilities. It is not known at present how to evaluate this possibility.

We note that high β, high bootstrap fraction, MHD stable profiles developed for the NSTX experiment [21] also have the same character as the VNS profiles. Thus, NSTX (and also MAST) are excellent test beds to examine the velocity shear stabilization physics. They have considerably more velocity shear than an $A = 3$ ignition device for drift and ITG modes; however, by running with current profiles which are not as optimal (*i.e.*, not as hollow), they can be reduced to qualitatively the same regime for velocity shear stabilization as $A = 3$.

Also note that the velocity shear in the NSTX case vanishes in the plasma at a point. This generic possibility can occur for a variety of pressure profiles. Since the velocity shear is less than the growth rate only over a small fraction of the profile, it is hoped that this would only result in localized turbulence which would not strongly affect global confinement. However a determination of the effect of nulls in the velocity shear must await a more self-consistent treatment.

The cases presented so far have emphasized core transport, but we note that similar considerations apply in the region of the H-mode pedestal. For model MHD equilibria generated by TOQ which include bootstrap current and with β values at the top of the pedestal in the range of $0.5\% - 1\%$, with a full width of 4% of the minor radius, the growth rates of drift and ITG modes are substantially reduced by β gradient effects, similar to fluid

calculations [23]. This makes the modes much easier to stabilize with velocity shear than had been previously indicated [24]. Without the bootstrap current, the pedestal would be ideal ballooning unstable in such cases. With the bootstrap current, the edge violates the "peeling mode" stability criterion. Balancing the velocity shear with an estimate of the ideal growth rate produces a pedestal beta scaling which goes as $\rho_*^{2/3}$, rather than ρ_*.

In experiments with velocity shear which exceeds the instability growth rate [3], ion and density transport drop to neoclassical levels. We now presume that this is true in our calculated cases, and that the high k microtearing modes are also stabilized in the outer region where their growth rates are much less than the velocity shearing rate, so that neoclassical transport results. These assumptions imply that very small ignited plasmas are possible at low aspect ratio.

The `NCLASS` [25] code was used to determine neoclassical transport in the transport code `NT`, using self-consistent equilibria computed by TOQ for high bootstrap fractions [20]. The heating source was given by the local fusion alpha energy production rate times a multiplier. To mimic the effect of the high k tearing modes, the assumption was made that the electron temperature was flattened inside of varying radii. Parameters characteristic of proposed volume neutron sources were used ($R = 0.7\mathrm{m}, B_T = 2\mathrm{T}, \kappa = 3$), where B_T is the vacuum field at the geometric center. 60 MW of fusion power is produced, and only 45% of the alpha power is needed to sustain ignition if the electron temperature is flattened over the inner 90% of the minor radius of the plasma.

The pressure profiles found in these cases are quite similar to profiles found to optimize MHD stability [20,21]. We believe that broad pressure profiles arise because of a feedback effect. The local aspect ratio scaling of neoclassical thermal conductivity implies that it is large in the center, leading to a low pressure gradient, which (because most of the current is bootstrap driven) further raises the safety factor in the center which further increases neoclassical transport in the center, *etc.* Central electron flattening from modes such as the microtearing mode produces further broadening.

In addition to being ideal MHD ballooning stable, arguments based on the shape fac-

tor [26] and initial calculations [22] are that the plasma can be stable to low n modes with a conducting wall. This is continuing to be investigated.

In conclusion, we find that small ignition devices are possible for plasmas with very hollow current profiles and low aspect ratio is particularly advantageous.

Acknowledgments

This work was funded by DOE. Computations were performed at NERSC, with partial support from DoE's Numerical Tokamak Turbulence Project.

REFERENCES

[1] E. J. Synakowski, Plasma Phys. and Control. Fusion **40**, 581 (1998).

[2] K. H. Burrell, Phys. Plasmas, **4**, 1499 (1997).

[3] G. M. Staebler, Plasma Phys. and Control. Fusion **40**, 569 (1998).

[4] M. A. Beer, *et al.*, Phys. Plasmas **4**, 1792 (1997).

[5] R. E. Waltz, Special Issue Phys. Plasmas, (1997).

[6] M. Kotschenreuther, *et al.*, Comput. Phys. Commun. **88**, 128 (1995).

[7] T. M. Antonsen, Jr. and B. Lane, Phys. Fluids **23**, 1205 (1980).

[8] R. L. Miller and J. W. Van Dam, Nucl. Fusion **28**, 2101 (1987).

[9] P. M. de Zeeuw, JCAM **33**, 1 (1990).

[10] R. Bell, *et al.*, This conference.

[11] K. C. Shaing *et al.*, Phys. Plasmas **3**, 965 (1996).

[12] M. Kotschenreuther, *et al.*, Phys. Plasmas **2**, 2381 (1995).

[13] G. Rewoldt and W. M. Tang, Phys. Plasmas **3**, 1667 (1996).

[14] J. M. Greene and M. S. Chance, Nucl. Fusion **21**, 453 (1981).

[15] C. M. Bishop *et al.*, Nucl. Fusion **24**, 1579 (1984).

[16] B. Dorland *et al.*, University of Maryland, Manuscript in preparation.

[17] H. L. Berk and R. R. Dominguez, J. Plasma Phys. **18**, 31 (1977).

[18] D. E. Hastings and J. E. McCune, Phys. Fluids **25**, 509 (1982).

[19] M. Fivaz, *et al.*, Phys. Rev. Lett. **78**, 3471 (1997).

[20] R. L. Miller, *et al.*, Phys. Plasmas **4**, 1062 (1997).

[21] J. Menard, *et al.*, Nuc. Fusion **37**, 595 (1997).

[22] J. Menard, private communication.

[23] B. Rogers, *et al.*, This conference.

[24] M. Kotschenreuther, *et al.*, IAEA Fusion Energy Conference proceedings, 1996.

[25] W. A. Houlberg *et al.*, Phys. Plasmas **4**, 3230 (1997).

[26] A. Turnbull, *et al.*, General Atomics report GA-A22324, accepted for publication.

[27] Y. Koida, *et al.*, Plasma Phys. and Control. Fusion **40**, 97 (1998).

FIGURE CAPTIONS

FIG. 1. Growth rates for L-mode like profiles *vs.* minor radius for cases with $A = 3$ and $A = 1.4$ for similar κ, δ, q_{95} and profile shapes.

FIG. 2. (a) Growth rates and (b) diamagnetic shearing rates *vs.* current profile hollowness for $A = 3$.

FIG. 3. (a) Growth rates and (b) diamagnetic shearing *vs.* current profile hollowness for $A = 1.4$. Note the different scale from $A = 3$ to display the larger core growth rates.

FIG. 4. (a) Growth rate and (b) mixing length diffusivity *vs.* equilibrium gradient for several values of $k_\theta \rho_i$.

FIG. 5. Growth rate and shearing rate *vs.* minor radius for high bootstrap fraction profiles, with (a) $A = 3$ (b) $A = 1.4$ and (c) NSTX.

FIGURES

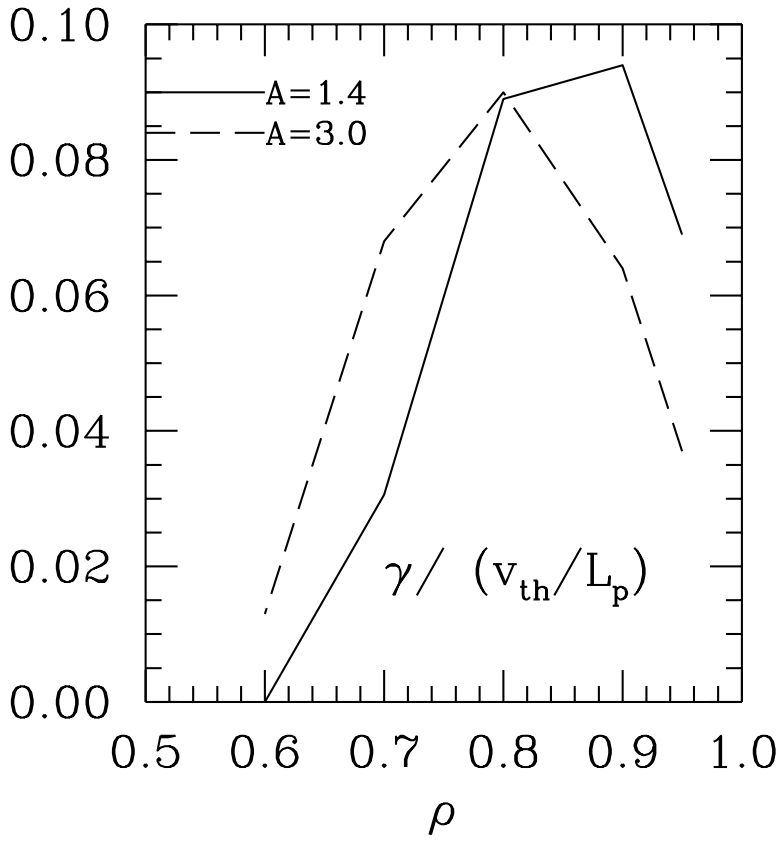

FIG. 1.

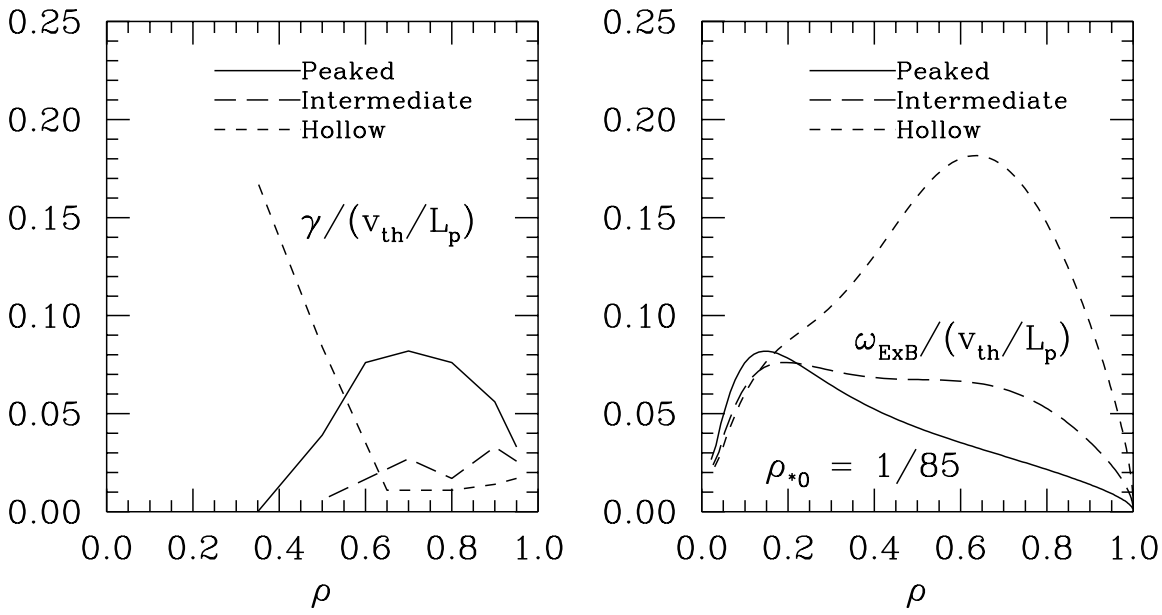
0.25
0.20
0.15
0.10
0.05
0.00
0.0
0.2
0.4
0.6
0.8
1.0
ρ
Peaked
Intermediate
Hollow
γ/(v_th/L_p)
ω_ExB/(v_th/L_p)
ρ_*0 = 1/85

FIG. 2.

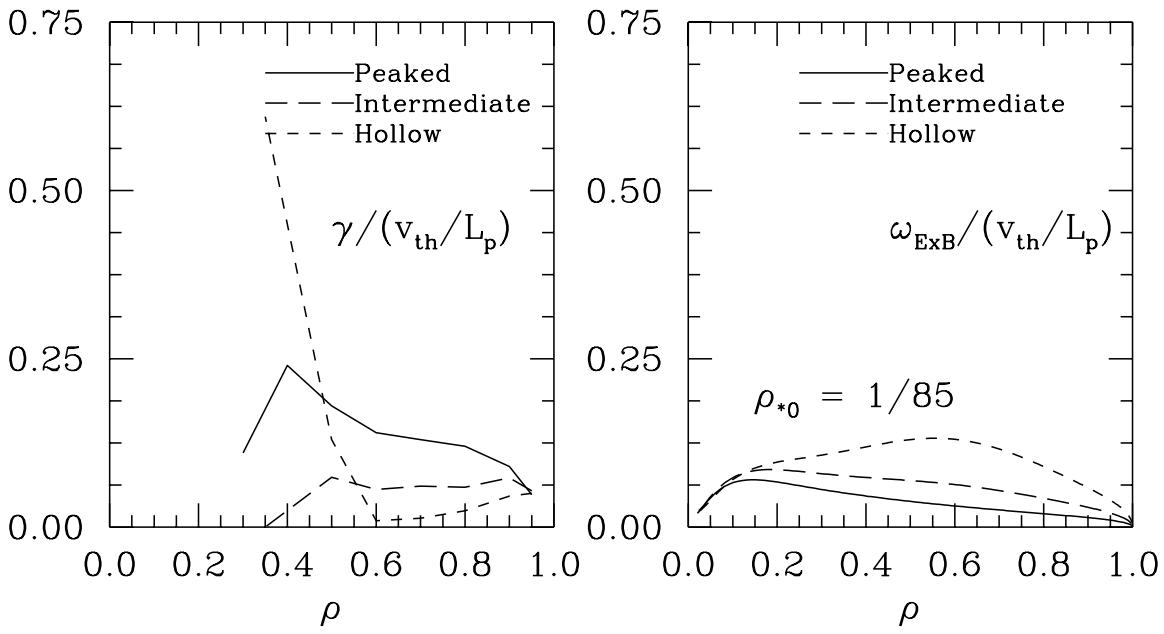
0.75
0.50
0.25
0.00
0.0
0.2
0.4
0.6
0.8
1.0
ρ
Peaked
Intermediate
Hollow
γ/(v_th/L_p)
ω_ExB/(v_th/L_p)
ρ_*0 = 1/85

FIG. 3.

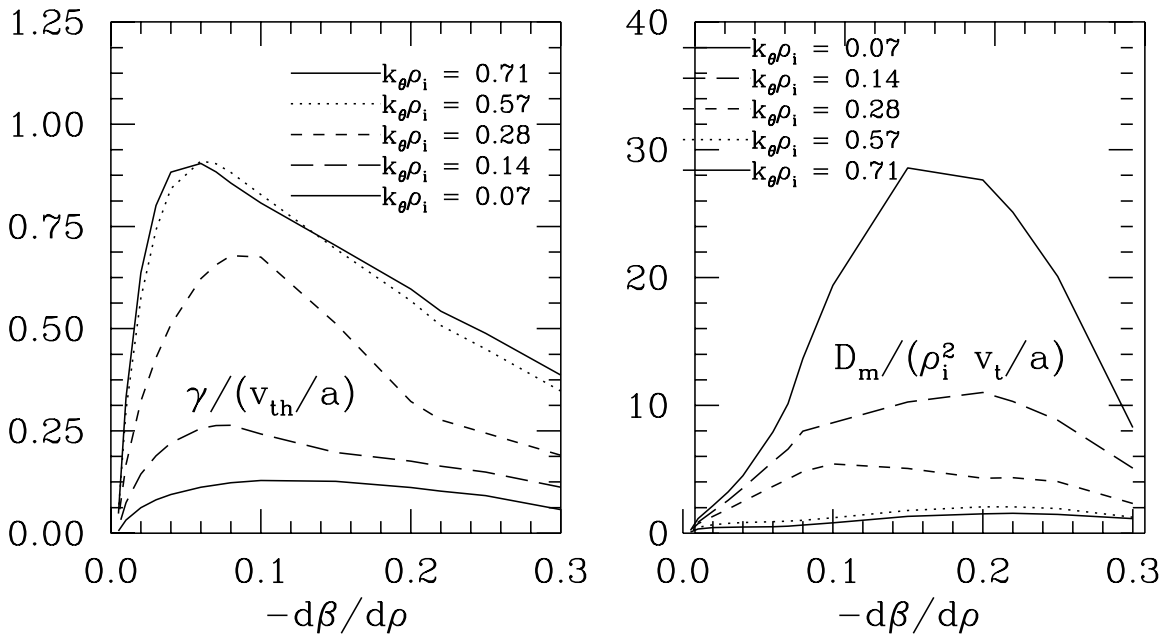
1.25
1.00
0.75
0.50
0.25
0.00
0.0
0.1
0.2
0.3
$-d\beta/d\rho$
$\gamma/(v_{th}/a)$
$k_\theta\rho_i$ = 0.71
$k_\theta\rho_i$ = 0.57
$k_\theta\rho_i$ = 0.28
$k_\theta\rho_i$ = 0.14
$k_\theta\rho_i$ = 0.07
40
30
20
10
0
$D_m/(\rho_i^2\ v_t/a)$

FIG. 4.

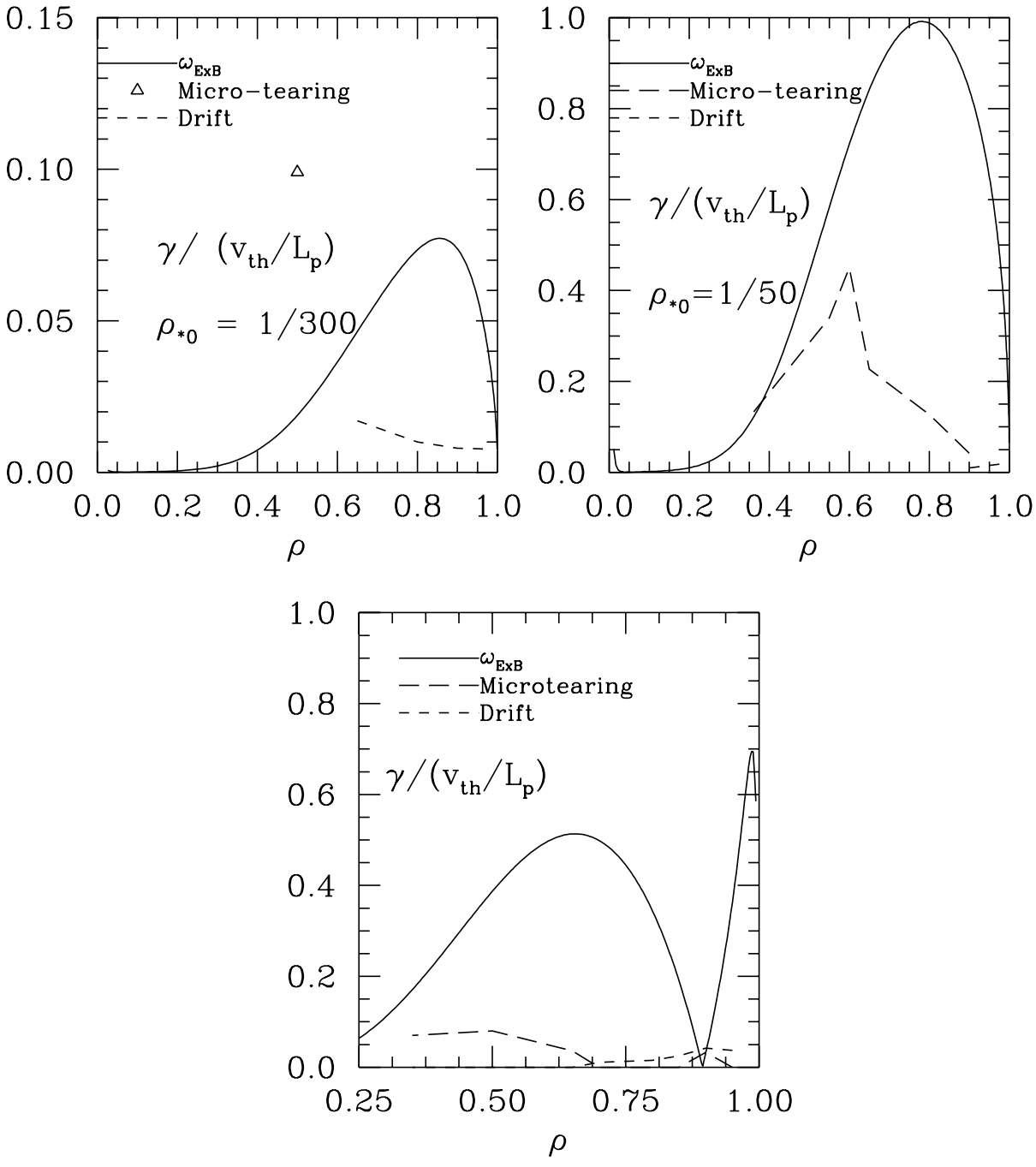
0.15
0.10
0.05
0.00
0.0
0.2
0.4
0.6
0.8
1.0
ρ
ω_ExB
Micro−tearing
Drift
γ/ (v_th/L_p)
ρ_*0 = 1/300
1.0
0.8
0.6
0.4
0.2
0.0
γ/(v_th/L_p)
ρ_*0=1/50
Microtearing
0.25
0.50
0.75
1.00

FIG. 5.